



CERN-EP-2016-294
 LHCb-PAPER-2016-050
 December 7, 2016

Observation of the decay

$$\Xi_b^- \rightarrow p K^- K^-$$

The LHCb collaboration[†]

Abstract

Decays of the Ξ_b^- and Ω_b^- baryons to the charmless final states $ph^-h'^-$, where $h^{(\prime)}$ denotes a kaon or pion, are searched for with the LHCb detector. The analysis is based on a sample of proton-proton collision data collected at centre-of-mass energies $\sqrt{s} = 7$ and 8 TeV , corresponding to an integrated luminosity of 3 fb^{-1} . The decay $\Xi_b^- \rightarrow p K^- K^-$ is observed with a significance of 8.7 standard deviations, and evidence at the level of 3.4 standard deviations is found for the $\Xi_b^- \rightarrow p K^- \pi^-$ decay. Results are reported, relative to the $B^- \rightarrow K^+ K^- K^-$ normalisation channel, for the products of branching fractions and b -hadron production fractions. The branching fractions of $\Xi_b^- \rightarrow p K^- \pi^-$ and $\Xi_b^- \rightarrow p \pi^- \pi^-$ relative to $\Xi_b^- \rightarrow p K^- K^-$ decays are also measured.

Published in Phys. Rev. Lett.

© CERN on behalf of the LHCb collaboration, licence CC-BY-4.0.

[†]Authors are listed at the end of this Letter.

Decays of b hadrons to final states that do not contain charm quarks provide fertile ground for studies of CP violation, *i.e.* the breaking of symmetry under the combined charge conjugation and parity operations. Significant asymmetries have been observed between B and \bar{B} partial widths in $\bar{B}^0 \rightarrow K^- \pi^+$ [1–4] and $\bar{B}_s^0 \rightarrow K^+ \pi^-$ [3, 4] decays. Even larger CP -violation effects have been observed in regions of the phase space of $B^- \rightarrow \pi^+ \pi^- \pi^-$, $K^- \pi^+ \pi^-$, $K^+ K^- K^-$ and $K^+ K^- \pi^-$ decays [5–7]. A number of theoretical approaches [8–18] have been proposed to determine whether the observed effects are consistent with being solely due to the non-zero phase in the quark mixing matrix [19, 20] of the Standard Model, or whether additional sources of asymmetry are contributing.

Breaking of the symmetry between matter and antimatter has not yet been observed with a significance of more than five standard deviations (σ) in the properties of any baryon. Recently, however, the first evidence of CP violation in the b -baryon sector has been reported from an analysis of $\Lambda_b^0 \rightarrow p \pi^- \pi^+ \pi^-$ decays [21]. Other CP -asymmetry parameters measured in Λ_b^0 baryon decays to $p \pi^-$, $p K^-$ [3], $K_s^0 p \pi^-$ [22], $\Lambda K^+ K^-$ and $\Lambda K^+ \pi^-$ [23] final states are consistent with zero within the current experimental precision; these comprise the only charmless hadronic b -baryon decays that have been observed to date. It is therefore of great interest to search for additional charmless b -baryon decays that may be used in future to investigate CP -violation effects.

In this Letter, the first search is presented for decays of Ξ_b^- and Ω_b^- baryons, with constituent quark contents of bsd and bss , to the charmless hadronic final states $ph^- h'^-$, where $h^{(\prime)}$ is a kaon or pion. The inclusion of charge-conjugate processes is implied throughout. Example decay diagrams for the $\Xi_b^- \rightarrow p K^- K^-$ mode are shown in Fig. 1. Interference between Cabibbo-suppressed tree and loop diagrams may lead to CP -violation effects. The $\Xi_b^- \rightarrow p K^- \pi^-$ and $\Omega_b^- \rightarrow p K^- K^-$ decays proceed by tree-level diagrams similar to that of Fig. 1 (left). Diagrams for $\Omega_b^- \rightarrow p K^- \pi^-$ and both Ξ_b^- and $\Omega_b^- \rightarrow p \pi^- \pi^-$ require additional weak interaction vertices. The rates of these decays are therefore expected to be further suppressed.

The analysis is based on a sample of proton-proton collision data, recorded by the LHCb experiment at centre-of-mass energies $\sqrt{s} = 7$ and 8 TeV, corresponding to 3 fb^{-1} of integrated luminosity. Since the fragmentation fractions, $f_{\Xi_b^-}$ and $f_{\Omega_b^-}$, which quantify the probabilities for a b quark to hadronise into these particular states, have not been determined, it is not possible to measure absolute branching fractions. Instead, the

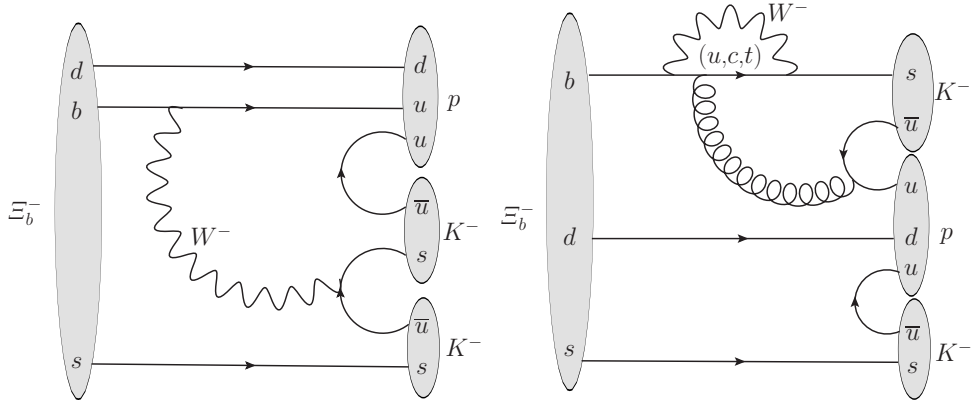


Figure 1: (Left) tree and (right) loop diagrams for the $\Xi_b^- \rightarrow p K^- K^-$ decay channel.

product of each branching fraction and the relevant fragmentation fraction is determined relative to the corresponding values for the topologically similar normalisation channel $B^- \rightarrow K^+ K^- K^-$ (the B^- fragmentation fraction is denoted f_u). Once one significant signal yield is observed, it becomes possible to determine ratios of branching fractions for decays of the same baryon to different final states, thus cancelling the dependence on the fragmentation fraction.

The LHCb detector [24, 25] is a single-arm forward spectrometer covering the pseudorapidity range $2 < \eta < 5$, designed for the study of particles containing b or c quarks. The pseudorapidity is defined as $-\ln [\tan(\theta/2)]$ where θ is the polar angle relative to the beam axis. The detector elements that are particularly relevant to this analysis are: a silicon-strip vertex detector surrounding the pp interaction region that allows b hadrons to be identified from their characteristically long flight distance; a tracking system that provides a measurement of the momentum (p) of charged particles; two ring-imaging Cherenkov detectors that enable different species of charged hadrons to be distinguished; and calorimeter and muon systems that provide information used for online event selection. Simulated data samples, produced with software described in Refs. [26–31], are used to evaluate the response of the detector to signal decays and to characterise the properties of certain types of background. These samples are generated separately for centre-of-mass energies of 7 and 8 TeV, simulating the corresponding data-taking conditions, and combined in appropriate quantities.

Online event selection is performed by a trigger [32] that consists of a hardware stage, based on information from the calorimeter and muon systems, followed by a software stage, which applies a full event reconstruction. At the hardware trigger stage, events are required to contain either a muon with high transverse momentum (p_T) or a particle that deposits high transverse energy in the calorimeters. For hadrons, the transverse energy threshold is typically 3.5 GeV. The software trigger for this analysis requires a two- or three-track secondary vertex with significant displacement from the primary pp interaction vertices (PVs). At least one charged particle must have p_T above a threshold of 1.7 (1.6) GeV/c in the $\sqrt{s} = 7$ (8) TeV data. This particle must also be inconsistent with originating from any PV as quantified through the difference in the vertex-fit χ^2 of a given PV reconstructed with and without the considered particle (χ^2_{IP}). A multivariate algorithm [33] is used for the identification of secondary vertices consistent with the decay of a b hadron.

The offline selection of b -hadron candidates formed from three tracks is carried out with an initial prefiltering stage, a requirement on the output of a neural network [34], and particle identification criteria. To avoid potential bias, the properties of candidates with invariant masses in windows around the Ξ_b^- and Ω_b^- masses were not inspected until after the analysis procedures were finalised. The prefiltering includes requirements on the quality, p , p_T and χ^2_{IP} of the tracks. Each b candidate must have a good quality vertex that is displaced from the closest PV (*i.e.* that with which it forms the smallest χ^2_{IP}), must satisfy p and p_T requirements, and must have reconstructed invariant mass loosely consistent with those of the b hadrons. A requirement is also imposed on the angle θ_{dir} between the b -candidate momentum vector and the line between the PV and the b -candidate decay vertex. In the offline selection, trigger signals are associated with reconstructed particles. Selection requirements can therefore be made not only on which trigger caused the event to be recorded, but also on whether the decision was due to the signal candidate or other particles produced in the pp collision [32]. Only candidates from

events with a hardware trigger caused by deposits of the signal in the calorimeter, or caused by other particles in the event, are retained. It is also required that the software trigger decision must have been caused by the signal candidate.

The inputs to the neural network for the final selection are the scalar sum of the p_T of all final-state tracks, the values of p_T and χ^2_{IP} for the highest p_T final-state track, the b -candidate $\cos(\theta_{\text{dir}})$, vertex χ^2 and χ^2_{IP} , together with a combination of momentum information and θ_{dir} that characterises how closely the momentum vector of the b candidate points back to the PV. The p_T asymmetry between the b candidate and other tracks within a circle, centred on the b candidate, with a radius $R = \sqrt{\delta\eta^2 + \delta\phi^2} < 1.5$ in the space of pseudorapidity and azimuthal angle ϕ (in radians) around the beam direction [35] is also used in the network. The distributions of these variables are consistent between simulated samples of signal decays and the $B^- \rightarrow K^+ K^- K^-$ normalisation channel, and between background-subtracted $B^- \rightarrow K^+ K^- K^-$ data and simulation. The neural network input variables are also found to be not strongly correlated with either the b -candidate mass or the position in the phase space of the decay. The neural network is trained to distinguish signal from combinatorial background in the $B^- \rightarrow K^+ K^- K^-$ channel, using a data-driven approach in which the two components are separated statistically using the *sPlot* method [36] with the b -candidate mass as discriminating variable. The requirement on the neural network output is optimised using a figure of merit [37] intended to give the best chance to observe the signal decays. The same neural network output requirement is made for all signal final states, and has an efficiency of about 60 %.

Using information from the ring-imaging Cherenkov detectors [38], criteria that identify uniquely the final-state tracks as either protons, pions or kaons are imposed, ensuring that no candidate appears in more than one of the final states considered. For pions and kaons these criteria are optimised simultaneously with that on the neural network output, using the same figure of merit. The desire to reject possible background from $B^- \rightarrow K^+ h^- h'^-$ in the signal modes justifies independent treatment of the proton identification requirement. In the simultaneous optimisation, the efficiency is taken from control samples while the expected background level is extrapolated from sidebands in the b -candidate mass distribution. The combined efficiency of the particle identification requirements is about 30 % for the $pK^- K^-$, 40 % for the $pK^- \pi^-$ and 50 % for the $p\pi^- \pi^-$ final state.

In order to ensure that any signal seen is due to charmless decays, candidates with pK^- invariant mass consistent with the $\Xi_b^- \rightarrow \Xi_c^0 h^- \rightarrow pK^- h^-$ or $\Xi_b^- \rightarrow \Xi_c^0 h^- \rightarrow p\pi^- h^-$ decay chain are vetoed. Similarly, candidates for the normalisation channel with $K^+ K^-$ invariant mass consistent with the $B^- \rightarrow D^0 K^- \rightarrow K^+ K^- K^-$ decay chain are removed. After all selection requirements are imposed, the fraction of selected events that contain more than one candidate is much less than 1 %; all such candidates are retained.

The yields of the signal decays are obtained from a simultaneous unbinned extended maximum likelihood fit to the b -candidate mass distributions in the three $ph^- h'^-$ final states. This approach allows potential cross-feed from one channel to another, due to particle misidentification, to be constrained according to the expected rates. The yield of the normalisation channel is determined from a separate fit to the $K^+ K^- K^-$ mass distribution.

Each signal component is modelled with the sum of two Crystal Ball (CB) functions [39] with shared parameters describing the core width and peak position and with non-Gaussian tails to both sides. The tail parameters and the relative normalisation of the CB functions are determined from simulation. A scale factor relating the width in data to that in

simulation is determined from the fit to the normalisation channel. In the fit to the signal modes the peak positions are fixed to the known Ξ_b^- and Ω_b^- masses [40–42]; the only free parameters associated with the signal components are the yields.

Cross-feed backgrounds from other decays to $ph^-h'^-$ final states are also modelled with the sum of two CB functions, with all shape parameters fixed according to simulation but the width scaled in the same way as signal components. Cross-feed backgrounds from $B^- \rightarrow K^+h^-h'^-$ decays are modelled, in the mass interval of the fit, by exponential functions with shape fixed according to simulation. The yields of all cross-feed backgrounds are constrained according to expectations based on the yield in the correctly reconstructed channel and the (mis-)identification probabilities determined from control samples.

In addition to signal and cross-feed backgrounds, components for partially reconstructed and combinatorial backgrounds are included in each final state. Partially reconstructed backgrounds arise due to b -hadron decays into final states similar to the signal, but with additional soft particles that are not reconstructed. Possible examples include $\Xi_b^- \rightarrow N^+h^-h'^- \rightarrow p\pi^0h^-h'^-$ and $\Xi_b^- \rightarrow pK^{*-}h^- \rightarrow pK^-\pi^0h^-$. Such decays are investigated with simulation and it is found that many of them have similar b -candidate mass distributions. The shapes of these backgrounds are therefore taken from $\Xi_b^- \rightarrow N^+h^-h'^- \rightarrow p\pi^0h^-h'^-$ simulation, with possible additional contributions considered as a source of systematic uncertainty. The shapes are modelled with an ARGUS function [43] convolved with a Gaussian function. The parameters of these functions are taken from simulation, except for the threshold of the ARGUS function, which is fixed to the known mass difference $m_{\Xi_b^-} - m_{\pi^0}$ [40, 44]. The combinatorial background is modelled by an exponential function with the shape parameter shared between the three final states. Possible differences in the shape between the different final states are considered as a source of systematic uncertainty. The free parameters of the fit are the signal and background yields, and the combinatorial background shape parameter. The stability of the fit is confirmed using ensembles of pseudoexperiments with different values of signal yields.

The results of the fits are shown in Fig. 2. The significance of each of the signals is determined from the change in likelihood when the corresponding yield is fixed to zero, with relevant sources of systematic uncertainty taken into account. The signals for $\Xi_b^- \rightarrow pK^-K^-$ and $pK^-\pi^-$ decays are found to have significance of 8.7σ and 3.4σ , respectively; each of the other signal modes has significance less than 2σ . The relative branching fractions multiplied by fragmentation fractions are determined as

$$R_{ph^-h'^-} \equiv \frac{f_{\Xi_b^-}}{f_u} \frac{\mathcal{B}(\Xi_b^- \rightarrow ph^-h'^-)}{\mathcal{B}(B^- \rightarrow K^+K^-K^-)} = \frac{\mathcal{N}(\Xi_b^- \rightarrow ph^-h'^-)}{\mathcal{N}(B^- \rightarrow K^+K^-K^-)} \frac{\epsilon(B^- \rightarrow K^+K^-K^-)}{\epsilon(\Xi_b^- \rightarrow ph^-h'^-)}, \quad (1)$$

where the yields \mathcal{N} are obtained from the fits. A similar expression is used for the Ω_b^- decay modes. The efficiencies ϵ are determined from simulation, weighted according to the most recent Ξ_b^- and Ω_b^- lifetime measurements [40–42], taking into account contributions from the detector geometry, reconstruction and both online and offline selection criteria. These are determined as a function of the position in phase space in each of the three-body final states. The phase space for each of the Ξ_b^- and Ω_b^- decays to $ph^-h'^-$ is five-dimensional, but significant variations in efficiency occur only in the variables that describe the Dalitz plot. Simulation is used to evaluate each contribution to the efficiency except for the effect of the particle identification criteria, which is determined from data control samples weighted according to the expected kinematics of the signal tracks [38, 45]. The description

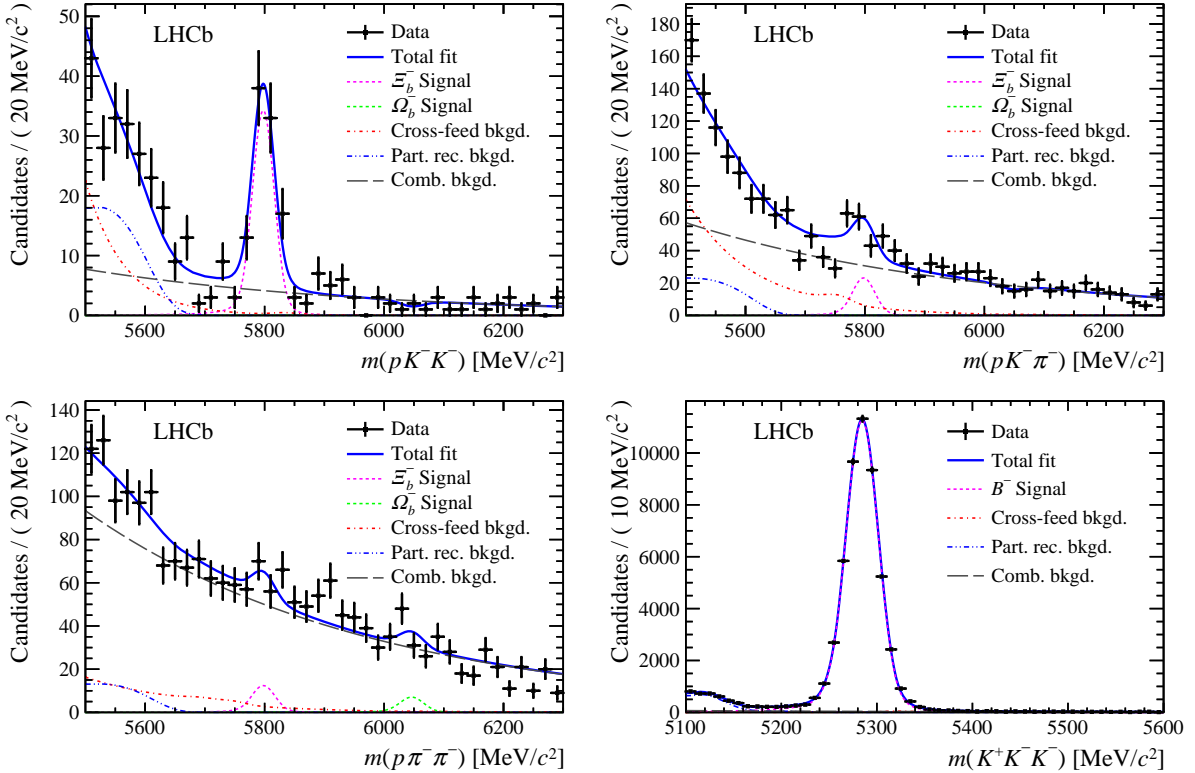


Figure 2: Mass distributions for b -hadron candidates in the (top left) pK^-K^- , (top right) $pK^-\pi^-$, (bottom left) $p\pi^-\pi^-$ and (bottom right) $K^+K^-K^-$ final states. Results of the fits are shown with dark blue solid lines. Signals for Ξ_b^- and $B^- (\Omega_b^-)$ decays are shown with pink (light green) dashed lines, combinatorial backgrounds are shown with grey long-dashed lines, cross-feed backgrounds are shown with red dot-dashed lines, and partially reconstructed backgrounds are shown with dark blue double-dot-dashed lines.

of reconstruction and selection efficiencies in the simulation has been validated with large control samples; the impact on the results of possible residual differences between data and simulation is negligible.

For the $\Xi_b^- \rightarrow pK^-K^-$, $\Xi_b^- \rightarrow pK^-\pi^-$ and $B^- \rightarrow K^+K^-K^-$ channels, efficiency corrections for each candidate are applied using the method of Ref. [46] to take the variation over the phase space into account. Using this procedure, the efficiency-corrected and background-subtracted $m(pK^-)_{\min}$ distribution shown in Fig. 3 is obtained from $\Xi_b^- \rightarrow pK^-K^-$ candidates. Here $m(pK^-)_{\min}$ indicates the smaller of the two $m(pK^-)$ values for each signal candidate, evaluated with the Ξ_b^- and the final-state particle masses fixed to their known values [40, 44]. The distribution contains a clear peak from the $\Lambda(1520)$ resonance, a structure that is consistent with being a combination of the $\Lambda(1670)$ and $\Lambda(1690)$ states, and possible additional contributions at higher mass. Compared to the pK^- structures seen in the amplitude analysis of $\Lambda_b^0 \rightarrow J/\psi pK^-$ [47], the contributions from the broad $\Lambda(1600)$ and $\Lambda(1810)$ states appear to be smaller. A detailed amplitude analysis will be of interest when larger samples are available.

For channels without significant signal yields the efficiency averaged over phase space is used in Eq. (1). A corresponding systematic uncertainty is assigned from the variation of the efficiency over the phase space; this is the dominant source of systematic uncertainty

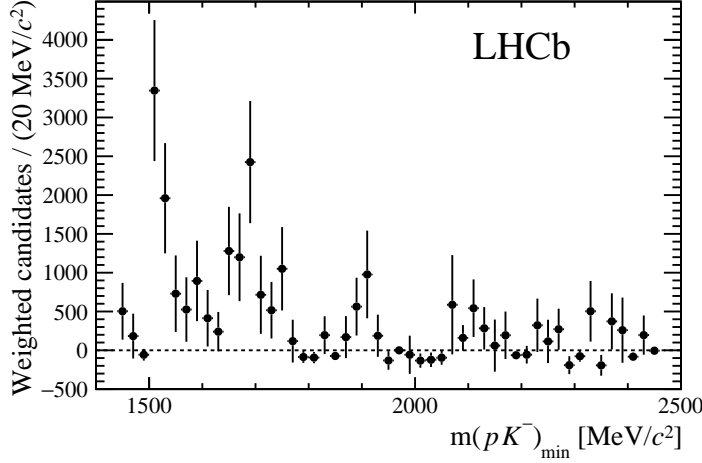


Figure 3: Efficiency-corrected and background-subtracted [36] $m(pK^-)_{\min}$ distribution from $\Xi_b^- \rightarrow pK^- K^-$ candidates.

Table 1: Fitted yields, efficiencies and relative branching fractions multiplied by fragmentation fractions ($R_{ph-h'}$). The two uncertainties quoted on $R_{ph-h'}$ are statistical and systematic. Upper limits are quoted at 90 (95) % confidence level for modes with signal significance less than 3σ . Uncertainties on the efficiencies are not given as only the relative uncertainties affect the branching fraction measurements.

Mode	Yield \mathcal{N}	Efficiency ϵ (%)	$R_{ph-h'} (10^{-5})$
$\Xi_b^- \rightarrow pK^- K^-$	82.9 ± 10.4	0.398	$265 \pm 35 \pm 47$
$\Xi_b^- \rightarrow pK^- \pi^-$	59.6 ± 16.0	0.293	$259 \pm 64 \pm 49$
$\Xi_b^- \rightarrow p\pi^- \pi^-$	33.2 ± 17.9	0.573	$74 \pm 40 \pm 36 < 147$ (166)
$\Omega_b^- \rightarrow pK^- K^-$	-2.8 ± 2.5	0.375	$-9 \pm 9 \pm 6 < 18$ (22)
$\Omega_b^- \rightarrow pK^- \pi^-$	-7.6 ± 9.2	0.418	$-23 \pm 28 \pm 23 < 51$ (62)
$\Omega_b^- \rightarrow p\pi^- \pi^-$	20.1 ± 13.8	0.536	$48 \pm 33 \pm 28 < 109$ (124)
$B^- \rightarrow K^+ K^- K^-$	$50\,490 \pm 250$	0.643	—

for those channels. The quantities entering Eq. (1), and the results for $R_{ph-h'}$, are reported in Table 1. When the signal significance is less than 3σ , upper limits are set by integrating the likelihood after multiplying by a prior probability distribution that is uniform in the region of positive branching fraction.

The sources of systematic uncertainty arise from the fit model and the knowledge of the efficiency. The fit model is changed by varying the fixed parameters of the model, using alternative shapes for the components, and by including components that are omitted in the baseline fit. Intrinsic biases in the fitted yields are investigated with simulated pseudoexperiments, and are found to be negligible. Uncertainties in the efficiency arise due to the limited size of the simulation samples and possible residual differences between data and simulation in the trigger and particle identification efficiencies [48]. Possible biases in the results due to the vetoes of charm hadrons are also accounted for. The efficiency depends on the signal decay-time distribution, and therefore the precision of the Ξ_b^- and Ω_b^- lifetime measurements [40–42] is a source of uncertainty. Similarly, the p_T distribution assumed for signal decays in the simulation affects the efficiency. Since the p_T spectra for

Ξ_b^- and Ω_b^- baryons produced in LHC collisions have not been measured, the effect is estimated by weighting simulation to the background-subtracted [36] p_T distribution for $\Xi_b^- \rightarrow pK^-K^-$ decays obtained from the data. The difference in the average efficiency between the weighted and unweighted simulation is assigned as the associated systematic uncertainty. This is the dominant source of systematic uncertainty for the $\Xi_b^- \rightarrow pK^-K^-$ and $\Xi_b^- \rightarrow pK^-\pi^-$ modes.

The yield of $\Xi_b^- \rightarrow pK^-K^-$ decays is sufficient to use as normalisation for the relative branching fractions of the other Ξ_b^- decays. The results are

$$\begin{aligned}\frac{\mathcal{B}(\Xi_b^- \rightarrow pK^-\pi^-)}{\mathcal{B}(\Xi_b^- \rightarrow pK^-K^-)} &= 0.98 \pm 0.27 \text{ (stat)} \pm 0.09 \text{ (syst)}, \\ \frac{\mathcal{B}(\Xi_b^- \rightarrow p\pi^-\pi^-)}{\mathcal{B}(\Xi_b^- \rightarrow pK^-K^-)} &= 0.28 \pm 0.16 \text{ (stat)} \pm 0.13 \text{ (syst)} < 0.56 \text{ (0.63)},\end{aligned}$$

where the upper limit is quoted at 90 (95) % confidence level. The same sources of systematic uncertainty as discussed above are considered. Since the effects due to the p_T distribution largely cancel, the dominant contributions are due to the trigger efficiency, fit model and (for the $\Xi_b^- \rightarrow p\pi^-\pi^-$ mode) efficiency variation across the phase space.

In summary, a search for decays of Ξ_b^- and Ω_b^- baryons to $ph^-h'^-$ final states has been carried out with a sample of proton-proton collision data corresponding to an integrated luminosity of 3 fb^{-1} . The first observation of the $\Xi_b^- \rightarrow pK^-K^-$ decay, and first evidence for the $\Xi_b^- \rightarrow pK^-\pi^-$ decay, have been obtained; there is no significant signal for the other modes. This is the first observation of a Ξ_b decay to a charmless final state. These modes may be used in future to search for CP asymmetries in the b -baryon sector.

Acknowledgements

We express our gratitude to our colleagues in the CERN accelerator departments for the excellent performance of the LHC. We thank the technical and administrative staff at the LHCb institutes. We acknowledge support from CERN and from the national agencies: CAPES, CNPq, FAPERJ and FINEP (Brazil); NSFC (China); CNRS/IN2P3 (France); BMBF, DFG and MPG (Germany); INFN (Italy); FOM and NWO (The Netherlands); MNiSW and NCN (Poland); MEN/IFA (Romania); MinES and FASO (Russia); MinECo (Spain); SNSF and SER (Switzerland); NASU (Ukraine); STFC (United Kingdom); NSF (USA). We acknowledge the computing resources that are provided by CERN, IN2P3 (France), KIT and DESY (Germany), INFN (Italy), SURF (The Netherlands), PIC (Spain), GridPP (United Kingdom), RRCKI and Yandex LLC (Russia), CSCS (Switzerland), IFIN-HH (Romania), CBPF (Brazil), PL-GRID (Poland) and OSC (USA). We are indebted to the communities behind the multiple open source software packages on which we depend. Individual groups or members have received support from AvH Foundation (Germany), EPLANET, Marie Skłodowska-Curie Actions and ERC (European Union), Conseil Général de Haute-Savoie, Labex ENIGMASS and OCEVU, Région Auvergne (France), RFBR and Yandex LLC (Russia), GVA, XuntaGal and GENCAT (Spain), Herchel Smith Fund, The Royal Society, Royal Commission for the Exhibition of 1851 and the Leverhulme Trust (United Kingdom).

References

- [1] BaBar collaboration, J. P. Lees *et al.*, *Measurement of CP asymmetries and branching fractions in charmless two-body B-meson decays to pions and kaons*, Phys. Rev. **D87** (2013) 052009, [arXiv:1206.3525](#).
- [2] Belle collaboration, Y.-T. Duh *et al.*, *Measurements of branching fractions and direct CP asymmetries for $B \rightarrow K\pi$, $B \rightarrow \pi\pi$ and $B \rightarrow KK$ decays*, Phys. Rev. **D87** (2013) 031103, [arXiv:1210.1348](#).
- [3] CDF collaboration, T. A. Aaltonen *et al.*, *Measurements of direct CP-violating asymmetries in charmless decays of bottom baryons*, Phys. Rev. Lett. **113** (2014) 242001, [arXiv:1403.5586](#).
- [4] LHCb collaboration, R. Aaij *et al.*, *First observation of CP violation in the decays of B_s^0 mesons*, Phys. Rev. Lett. **110** (2013) 221601, [arXiv:1304.6173](#).
- [5] LHCb collaboration, R. Aaij *et al.*, *Measurement of CP violation in the phase space of $B^\pm \rightarrow K^\pm \pi^+ \pi^-$ and $B^\pm \rightarrow K^\pm K^+ K^-$ decays*, Phys. Rev. Lett. **111** (2013) 101801, [arXiv:1306.1246](#).
- [6] LHCb collaboration, R. Aaij *et al.*, *Measurement of CP violation in the phase space of $B^\pm \rightarrow K^+ K^- \pi^\pm$ and $B^\pm \rightarrow \pi^+ \pi^- \pi^\pm$ decays*, Phys. Rev. Lett. **112** (2014) 011801, [arXiv:1310.4740](#).
- [7] LHCb collaboration, R. Aaij *et al.*, *Measurement of CP violation in the three-body phase space of charmless B^\pm decays*, Phys. Rev. **D90** (2014) 112004, [arXiv:1408.5373](#).
- [8] M. Gronau and J. L. Rosner, *Implications for CP asymmetries of improved data on $B \rightarrow K^0 \pi^0$* , Phys. Lett. **B666** (2008) 467, [arXiv:0807.3080](#).
- [9] S. Baek *et al.*, *Diagnostic for new physics in $B \rightarrow \pi K$ decays*, Phys. Lett. **B678** (2009) 97, [arXiv:0905.1495](#).
- [10] M. Ciuchini, M. Pierini, and L. Silvestrini, *New bounds on the CKM matrix from $B \rightarrow K\pi\pi$ Dalitz plot analyses*, Phys. Rev. **D74** (2006) 051301, [arXiv:hep-ph/0601233](#).
- [11] M. Ciuchini, M. Pierini, and L. Silvestrini, *Hunting the CKM weak phase with time-integrated Dalitz analyses of $B_s^0 \rightarrow KK\pi$ and $B_s^0 \rightarrow K\pi\pi$ decays*, Phys. Lett. **B645** (2007) 201, [arXiv:hep-ph/0602207](#).
- [12] M. Gronau, D. Pirjol, A. Soni, and J. Zupan, *Improved method for CKM constraints in charmless three-body B and B_s^0 decays*, Phys. Rev. **D75** (2007) 014002, [arXiv:hep-ph/0608243](#).
- [13] M. Gronau, D. Pirjol, A. Soni, and J. Zupan, *Constraint on $\bar{\rho}, \bar{\eta}$ from $B \rightarrow K^* \pi$* , Phys. Rev. **D77** (2008) 057504, [arXiv:0712.3751](#).
- [14] I. Bediaga, G. Guerrer, and J. M. de Miranda, *Extracting the quark mixing phase γ from $B^\pm \rightarrow K^\pm \pi^+ \pi^-$, $B^0 \rightarrow K_s^0 \pi^+ \pi^-$, and $\bar{B}^0 \rightarrow K_s^0 \pi^+ \pi^-$* , Phys. Rev. **D76** (2007) 073011, [arXiv:hep-ph/0608268](#).

- [15] M. Gronau, D. Pirjol, and J. Zupan, *CP asymmetries in $B \rightarrow K\pi, K^*\pi, \rho K$ decays*, Phys. Rev. **D81** (2010) 094011, [arXiv:1001.0702](#).
- [16] M. Gronau, D. Pirjol, and J. L. Rosner, *Calculating phases between $B \rightarrow K^*\pi$ amplitudes*, Phys. Rev. **D81** (2010) 094026, [arXiv:1003.5090](#).
- [17] M. Imbeault, N. R.-L. Lorier, and D. London, *Measuring γ in $B \rightarrow K\pi\pi$ decays*, Phys. Rev. **D84** (2011) 034041, [arXiv:1011.4973](#).
- [18] B. Bhattacharya and D. London, *Using U-spin to extract γ from charmless $B \rightarrow PPP$ decays*, JHEP **04** (2015) 154, [arXiv:1503.00737](#).
- [19] N. Cabibbo, *Unitary symmetry and leptonic decays*, Phys. Rev. Lett. **10** (1963) 531.
- [20] M. Kobayashi and T. Maskawa, *CP violation in the renormalizable theory of weak interaction*, Prog. Theor. Phys. **49** (1973) 652.
- [21] LHCb collaboration, R. Aaij *et al.*, *Probing matter-antimatter asymmetries in beauty baryon decays*, Nature Physics (2017) , [arXiv:1609.05216](#).
- [22] LHCb collaboration, R. Aaij *et al.*, *Searches for Λ_b^0 and Ξ_b^0 decays to $K_s^0 p \pi^-$ and $K_s^0 p K^-$ final states with first observation of the $\Lambda_b^0 \rightarrow K_s^0 p \pi^-$ decay*, JHEP **04** (2014) 087, [arXiv:1402.0770](#).
- [23] LHCb collaboration, R. Aaij *et al.*, *Observations of $\Lambda_b^0 \rightarrow \Lambda K^+ \pi^-$ and $\Lambda_b^0 \rightarrow \Lambda K^+ K^-$ decays and searches for other Λ_b^0 and Ξ_b^0 decays to $\Lambda h^+ h^-$ final states*, JHEP **05** (2016) 081, [arXiv:1603.00413](#).
- [24] LHCb collaboration, A. A. Alves Jr. *et al.*, *The LHCb detector at the LHC*, JINST **3** (2008) S08005.
- [25] LHCb collaboration, R. Aaij *et al.*, *LHCb detector performance*, Int. J. Mod. Phys. **A30** (2015) 1530022, [arXiv:1412.6352](#).
- [26] T. Sjöstrand, S. Mrenna, and P. Skands, *PYTHIA 6.4 physics and manual*, JHEP **05** (2006) 026, [arXiv:hep-ph/0603175](#); T. Sjöstrand, S. Mrenna, and P. Skands, *A brief introduction to PYTHIA 8.1*, Comput. Phys. Commun. **178** (2008) 852, [arXiv:0710.3820](#).
- [27] I. Belyaev *et al.*, *Handling of the generation of primary events in Gauss, the LHCb simulation framework*, J. Phys. Conf. Ser. **331** (2011) 032047.
- [28] D. J. Lange, *The EvtGen particle decay simulation package*, Nucl. Instrum. Meth. **A462** (2001) 152.
- [29] P. Golonka and Z. Was, *PHOTOS Monte Carlo: A precision tool for QED corrections in Z and W decays*, Eur. Phys. J. **C45** (2006) 97, [arXiv:hep-ph/0506026](#).
- [30] Geant4 collaboration, J. Allison *et al.*, *Geant4 developments and applications*, IEEE Trans. Nucl. Sci. **53** (2006) 270; Geant4 collaboration, S. Agostinelli *et al.*, *Geant4: A simulation toolkit*, Nucl. Instrum. Meth. **A506** (2003) 250.

- [31] M. Clemencic *et al.*, *The LHCb simulation application, Gauss: Design, evolution and experience*, J. Phys. Conf. Ser. **331** (2011) 032023.
- [32] R. Aaij *et al.*, *The LHCb trigger and its performance in 2011*, JINST **8** (2013) P04022, [arXiv:1211.3055](https://arxiv.org/abs/1211.3055).
- [33] V. V. Gligorov and M. Williams, *Efficient, reliable and fast high-level triggering using a bonsai boosted decision tree*, JINST **8** (2013) P02013, [arXiv:1210.6861](https://arxiv.org/abs/1210.6861).
- [34] M. Feindt and U. Kerzel, *The NeuroBayes neural network package*, Nucl. Instrum. Meth. **A559** (2006) 190.
- [35] LHCb collaboration, R. Aaij *et al.*, *Observation of CP violation in $B^\pm \rightarrow DK^\pm$ decays*, Phys. Lett. **B712** (2012) 203, Erratum ibid. **B713** (2012) 351, [arXiv:1203.3662](https://arxiv.org/abs/1203.3662).
- [36] M. Pivk and F. R. Le Diberder, *sPlot: A statistical tool to unfold data distributions*, Nucl. Instrum. Meth. **A555** (2005) 356, [arXiv:physics/0402083](https://arxiv.org/abs/physics/0402083).
- [37] G. Punzi, *Sensitivity of searches for new signals and its optimization*, in *Statistical Problems in Particle Physics, Astrophysics, and Cosmology* (L. Lyons, R. Mount, and R. Reitmeyer, eds.), p. 79, 2003. [arXiv:physics/0308063](https://arxiv.org/abs/physics/0308063).
- [38] M. Adinolfi *et al.*, *Performance of the LHCb RICH detector at the LHC*, Eur. Phys. J. **C73** (2013) 2431, [arXiv:1211.6759](https://arxiv.org/abs/1211.6759).
- [39] T. Skwarnicki, *A study of the radiative cascade transitions between the Upsilon-prime and Upsilon resonances*, PhD thesis, Institute of Nuclear Physics, Krakow, 1986, DESY-F31-86-02.
- [40] LHCb collaboration, R. Aaij *et al.*, *Precision measurement of the mass and lifetime of the Ξ_b^- baryon*, Phys. Rev. Lett. **113** (2014) 242002, [arXiv:1409.8568](https://arxiv.org/abs/1409.8568).
- [41] LHCb collaboration, R. Aaij *et al.*, *Measurements of the mass and lifetime of the Ω_b^- baryon*, Phys. Rev. **D93** (2016) 092007, [arXiv:1604.01412](https://arxiv.org/abs/1604.01412).
- [42] Heavy Flavor Averaging Group, Y. Amhis *et al.*, *Averages of b-hadron, c-hadron, and τ -lepton properties as of summer 2014*, [arXiv:1412.7515](https://arxiv.org/abs/1412.7515), updated results and plots available at <http://www.slac.stanford.edu/xorg/hfag/>.
- [43] ARGUS collaboration, H. Albrecht *et al.*, *Search for hadronic $b \rightarrow u$ decays*, Phys. Lett. **B241** (1990) 278.
- [44] Particle Data Group, K. A. Olive *et al.*, *Review of particle physics*, Chin. Phys. **C38** (2014) 090001, and 2015 update.
- [45] L. Anderlini *et al.*, *The PIDCalib package*, LHCb-PUB-2016-021.
- [46] LHCb collaboration, R. Aaij *et al.*, *Observation of $B^0 \rightarrow \bar{D}^0 K^+ K^-$ and evidence for $B_s^0 \rightarrow \bar{D}^0 K^+ K^-$* , Phys. Rev. Lett. **109** (2012) 131801, [arXiv:1207.5991](https://arxiv.org/abs/1207.5991).
- [47] LHCb collaboration, R. Aaij *et al.*, *Observation of $J/\psi p$ resonances consistent with pentaquark states in $\Lambda_b^0 \rightarrow J/\psi p K^-$ decays*, Phys. Rev. Lett. **115** (2015) 072001, [arXiv:1507.03414](https://arxiv.org/abs/1507.03414).

- [48] LHCb collaboration, R. Aaij *et al.*, *Dalitz plot analysis of $B_s^0 \rightarrow \bar{D}^0 K^- \pi^+$ decays*, Phys. Rev. **D90** (2014) 072003, arXiv:1407.7712.

LHCb collaboration

R. Aaij⁴⁰, B. Adeva³⁹, M. Adinolfi⁴⁸, Z. Ajaltouni⁵, S. Akar⁵⁹, J. Albrecht¹⁰, F. Alessio⁴⁰, M. Alexander⁵³, S. Ali⁴³, G. Alkhazov³¹, P. Alvarez Cartelle⁵⁵, A.A. Alves Jr⁵⁹, S. Amato², S. Amerio²³, Y. Amhis⁷, L. An³, L. Anderlini¹⁸, G. Andreassi⁴¹, M. Andreotti^{17,g}, J.E. Andrews⁶⁰, R.B. Appleby⁵⁶, F. Archilli⁴³, P. d'Argent¹², J. Arnau Romeu⁶, A. Artamonov³⁷, M. Artuso⁶¹, E. Aslanides⁶, G. Auriemma²⁶, M. Baalouch⁵, I. Babuschkin⁵⁶, S. Bachmann¹², J.J. Back⁵⁰, A. Badalov³⁸, C. Baesso⁶², S. Baker⁵⁵, V. Balagura^{7,c}, W. Baldini¹⁷, R.J. Barlow⁵⁶, C. Barschel⁴⁰, S. Barsuk⁷, W. Barter⁴⁰, M. Baszczyk²⁷, V. Batozskaya²⁹, B. Batsukh⁶¹, V. Battista⁴¹, A. Bay⁴¹, L. Beaucourt⁴, J. Beddow⁵³, F. Bedeschi²⁴, I. Bediaga¹, L.J. Bel⁴³, V. Bellee⁴¹, N. Belloli^{21,i}, K. Belous³⁷, I. Belyaev³², E. Ben-Haim⁸, G. Bencivenni¹⁹, S. Benson⁴³, A. Berezhnoy³³, R. Bernet⁴², A. Bertolin²³, C. Betancourt⁴², F. Betti¹⁵, M.-O. Bettler⁴⁰, M. van Beuzekom⁴³, Ia. Bezshyiko⁴², S. Bifani⁴⁷, P. Billoir⁸, T. Bird⁵⁶, A. Birnkraut¹⁰, A. Bitadze⁵⁶, A. Bizzeti^{18,u}, T. Blake⁵⁰, F. Blanc⁴¹, J. Blouw^{11,†}, S. Blusk⁶¹, V. Bocci²⁶, T. Boettcher⁵⁸, A. Bondar^{36,w}, N. Bondar^{31,40}, W. Bonivento¹⁶, I. Bordyuzhin³², A. Borgheresi^{21,i}, S. Borghi⁵⁶, M. Borisjak³⁵, M. Borsato³⁹, F. Bossu⁷, M. Boubdir⁹, T.J.V. Bowcock⁵⁴, E. Bowen⁴², C. Bozzi^{17,40}, S. Braun¹², M. Britsch¹², T. Britton⁶¹, J. Brodzicka⁵⁶, E. Buchanan⁴⁸, C. Burr⁵⁶, A. Bursche², J. Buytaert⁴⁰, S. Cadeddu¹⁶, R. Calabrese^{17,g}, M. Calvi^{21,i}, M. Calvo Gomez^{38,m}, A. Camboni³⁸, P. Campana¹⁹, D.H. Campora Perez⁴⁰, L. Capriotti⁵⁶, A. Carbone^{15,e}, G. Carboni^{25,j}, R. Cardinale^{20,h}, A. Cardini¹⁶, P. Carniti^{21,i}, L. Carson⁵², K. Carvalho Akiba², G. Casse⁵⁴, L. Cassina^{21,i}, L. Castillo Garcia⁴¹, M. Cattaneo⁴⁰, G. Cavallero²⁰, R. Cenci^{24,t}, D. Chamont⁷, M. Charles⁸, Ph. Charpentier⁴⁰, G. Chatzikonstantinidis⁴⁷, M. Chefdeville⁴, S. Chen⁵⁶, S.-F. Cheung⁵⁷, V. Chobanova³⁹, M. Chrzaszcz^{42,27}, X. Cid Vidal³⁹, G. Ciezarek⁴³, P.E.L. Clarke⁵², M. Clemencic⁴⁰, H.V. Cliff⁴⁹, J. Closier⁴⁰, V. Coco⁵⁹, J. Cogan⁶, E. Cogneras⁵, V. Cogoni^{16,40,f}, L. Cojocariu³⁰, G. Collazuol^{23,o}, P. Collins⁴⁰, A. Comerma-Montells¹², A. Contu⁴⁰, A. Cook⁴⁸, G. Coombs⁴⁰, S. Coquereau³⁸, G. Corti⁴⁰, M. Corvo^{17,g}, C.M. Costa Sobral⁵⁰, B. Couturier⁴⁰, G.A. Cowan⁵², D.C. Craik⁵², A. Crocombe⁵⁰, M. Cruz Torres⁶², S. Cunliffe⁵⁵, R. Currie⁵⁵, C. D'Ambrosio⁴⁰, F. Da Cunha Marinho², E. Dall'Occo⁴³, J. Dalseno⁴⁸, P.N.Y. David⁴³, A. Davis³, K. De Bruyn⁶, S. De Capua⁵⁶, M. De Cian¹², J.M. De Miranda¹, L. De Paula², M. De Serio^{14,d}, P. De Simone¹⁹, C.-T. Dean⁵³, D. Decamp⁴, M. Deckenhoff¹⁰, L. Del Buono⁸, M. Demmer¹⁰, A. Dendek²⁸, D. Derkach³⁵, O. Deschamps⁵, F. Dettori⁴⁰, B. Dey²², A. Di Canto⁴⁰, H. Dijkstra⁴⁰, F. Dordei⁴⁰, M. Dorigo⁴¹, A. Dosil Suárez³⁹, A. Dovbnya⁴⁵, K. Dreimanis⁵⁴, L. Dufour⁴³, G. Dujany⁵⁶, K. Dungs⁴⁰, P. Durante⁴⁰, R. Dzhelyadin³⁷, A. Dziurda⁴⁰, A. Dzyuba³¹, N. Déléage⁴, S. Easo⁵¹, M. Ebert⁵², U. Egede⁵⁵, V. Egorychev³², S. Eidelman^{36,w}, S. Eisenhardt⁵², U. Eitschberger¹⁰, R. Ekelhof¹⁰, L. Eklund⁵³, S. Ely⁶¹, S. Esen¹², H.M. Evans⁴⁹, T. Evans⁵⁷, A. Falabella¹⁵, N. Farley⁴⁷, S. Farry⁵⁴, R. Fay⁵⁴, D. Fazzini^{21,i}, D. Ferguson⁵², A. Fernandez Prieto³⁹, F. Ferrari^{15,40}, F. Ferreira Rodrigues², M. Ferro-Luzzi⁴⁰, S. Filippov³⁴, R.A. Fini¹⁴, M. Fiore^{17,g}, M. Fiorini^{17,g}, M. Firlej²⁸, C. Fitzpatrick⁴¹, T. Fiutowski²⁸, F. Fleuret^{7,b}, K. Fohl⁴⁰, M. Fontana^{16,40}, F. Fontanelli^{20,h}, D.C. Forshaw⁶¹, R. Forty⁴⁰, V. Franco Lima⁵⁴, M. Frank⁴⁰, C. Frei⁴⁰, J. Fu^{22,q}, W. Funk⁴⁰, E. Furfarò^{25,j}, C. Färber⁴⁰, A. Gallas Torreira³⁹, D. Galli^{15,e}, S. Gallorini²³, S. Gambetta⁵², M. Gandelman², P. Gandini⁵⁷, Y. Gao³, L.M. Garcia Martin⁶⁹, J. García Pardiñas³⁰, J. Garra Tico⁴⁹, L. Garrido³⁸, P.J. Garsed⁴⁹, D. Gascon³⁸, C. Gaspar⁴⁰, L. Gavardi¹⁰, G. Gazzoni⁵, D. Gerick¹², E. Gersabeck¹², M. Gersabeck⁵⁶, T. Gershon⁵⁰, Ph. Ghez⁴, S. Gianì⁴¹, V. Gibson⁴⁹, O.G. Girard⁴¹, L. Giubega³⁰, K. Gizzov⁵², V.V. Gligorov⁸, D. Golubkov³², A. Golutvin^{55,40}, A. Gomes^{1,a}, I.V. Gorelov³³, C. Gotti^{21,i}, R. Graciani Diaz³⁸, L.A. Granado Cardoso⁴⁰, E. Graugés³⁸, E. Graverini⁴², G. Graziani¹⁸, A. Grecu³⁰, P. Griffith⁴⁷, L. Grillo^{21,40,i}, B.R. Gruberg Cazon⁵⁷, O. Grünberg⁶⁷, E. Gushchin³⁴, Yu. Guz³⁷, T. Gys⁴⁰, C. Göbel⁶², T. Hadavizadeh⁵⁷, C. Hadjivasiliou⁵, G. Haefeli⁴¹, C. Haen⁴⁰, S.C. Haines⁴⁹,

S. Hall⁵⁵, B. Hamilton⁶⁰, X. Han¹², S. Hansmann-Menzemer¹², N. Harnew⁵⁷, S.T. Harnew⁴⁸,
 J. Harrison⁵⁶, M. Hatch⁴⁰, J. He⁶³, T. Head⁴¹, A. Heister⁹, K. Hennessy⁵⁴, P. Henrard⁵,
 L. Henry⁸, E. van Herwijnen⁴⁰, M. Heß⁶⁷, A. Hicheur², D. Hill⁵⁷, C. Hombach⁵⁶, H. Hopchev⁴¹,
 W. Hulsbergen⁴³, T. Humair⁵⁵, M. Hushchyn³⁵, D. Hutchcroft⁵⁴, M. Idzik²⁸, P. Ilten⁵⁸,
 R. Jacobsson⁴⁰, A. Jaeger¹², J. Jalocha⁵⁷, E. Jans⁴³, A. Jawahery⁶⁰, F. Jiang³, M. John⁵⁷,
 D. Johnson⁴⁰, C.R. Jones⁴⁹, C. Joram⁴⁰, B. Jost⁴⁰, N. Jurik⁵⁷, S. Kandybei⁴⁵, M. Karacson⁴⁰,
 J.M. Kariuki⁴⁸, S. Karodia⁵³, M. Kecke¹², M. Kelsey⁶¹, M. Kenzie⁴⁹, T. Ketel⁴⁴,
 E. Khairullin³⁵, B. Khanji¹², C. Khurewathanakul⁴¹, T. Kirn⁹, S. Klaver⁵⁶, K. Klimaszewski²⁹,
 S. Koliiev⁴⁶, M. Kolpin¹², I. Komarov⁴¹, R.F. Koopman⁴⁴, P. Koppenburg⁴³, A. Kosmyntseva³²,
 A. Kozachuk³³, M. Kozeiha⁵, L. Kravchuk³⁴, K. Kreplin¹², M. Kreps⁵⁰, P. Krokovny^{36,w},
 F. Kruse¹⁰, W. Krzemien²⁹, W. Kuczewicz^{27,l}, M. Kucharczyk²⁷, V. Kudryavtsev^{36,w},
 A.K. Kuonen⁴¹, K. Kurek²⁹, T. Kvaratskheliya^{32,40}, D. Lacarrere⁴⁰, G. Lafferty⁵⁶, A. Lai¹⁶,
 G. Lanfranchi¹⁹, C. Langenbruch⁹, T. Latham⁵⁰, C. Lazzeroni⁴⁷, R. Le Gac⁶, J. van Leerdam⁴³,
 A. Leflat^{33,40}, J. Lefrançois⁷, R. Lefèvre⁵, F. Lemaitre⁴⁰, E. Lemos Cid³⁹, O. Leroy⁶,
 T. Lesiak²⁷, B. Leverington¹², T. Li³, Y. Li⁷, T. Likhomanenko^{35,68}, R. Lindner⁴⁰, C. Linn⁴⁰,
 F. Lionetto⁴², X. Liu³, D. Loh⁵⁰, I. Longstaff⁵³, J.H. Lopes², D. Lucchesi^{23,o},
 M. Lucio Martinez³⁹, H. Luo⁵², A. Lupato²³, E. Luppi^{17,g}, O. Lupton⁴⁰, A. Lusiani²⁴, X. Lyu⁶³,
 F. Machefert⁷, F. Maciuc³⁰, O. Maev³¹, K. Maguire⁵⁶, S. Malde⁵⁷, A. Malinin⁶⁸, T. Maltsev³⁶,
 G. Manca^{16,f}, G. Mancinelli⁶, P. Manning⁶¹, J. Maratas^{5,v}, J.F. Marchand⁴, U. Marconi¹⁵,
 C. Marin Benito³⁸, M. Marinangeli⁴¹, P. Marino^{24,t}, J. Marks¹², G. Martellotti²⁶, M. Martin⁶,
 M. Martinelli⁴¹, D. Martinez Santos³⁹, F. Martinez Vidal⁶⁹, D. Martins Tostes²,
 L.M. Massacrier⁷, A. Massafferri¹, R. Matev⁴⁰, A. Mathad⁵⁰, Z. Mathe⁴⁰, C. Matteuzzi²¹,
 A. Mauri⁴², E. Maurice^{7,b}, B. Maurin⁴¹, A. Mazurov⁴⁷, M. McCann^{55,40}, A. McNab⁵⁶,
 R. McNulty¹³, B. Meadows⁵⁹, F. Meier¹⁰, M. Meissner¹², D. Melnychuk²⁹, M. Merk⁴³,
 A. Merli^{22,q}, E. Michelin²³, D.A. Milanes⁶⁶, M.-N. Minard⁴, D.S. Mitzel¹², A. Mogini⁸,
 J. Molina Rodriguez¹, I.A. Monroy⁶⁶, S. Monteil⁵, M. Morandin²³, P. Morawski²⁸, A. Mordà⁶,
 M.J. Morello^{24,t}, O. Morgunova⁶⁸, J. Moron²⁸, A.B. Morris⁵², R. Mountain⁶¹, F. Muheim⁵²,
 M. Mulder⁴³, M. Mussini¹⁵, D. Müller⁵⁶, J. Müller¹⁰, K. Müller⁴², V. Müller¹⁰, P. Naik⁴⁸,
 T. Nakada⁴¹, R. Nandakumar⁵¹, A. Nandi⁵⁷, I. Nasteva², M. Needham⁵², N. Neri²²,
 S. Neubert¹², N. Neufeld⁴⁰, M. Neuner¹², T.D. Nguyen⁴¹, C. Nguyen-Mau^{41,n}, S. Nieswand⁹,
 R. Niet¹⁰, N. Nikitin³³, T. Nikodem¹², A. Nogay⁶⁸, A. Novoselov³⁷, D.P. O'Hanlon⁵⁰,
 A. Oblakowska-Mucha²⁸, V. Obraztsov³⁷, S. Ogilvy¹⁹, R. Oldeman^{16,f}, C.J.G. Onderwater⁷⁰,
 J.M. Otalora Goicochea², A. Otto⁴⁰, P. Owen⁴², A. Oyanguren⁶⁹, P.R. Pais⁴¹, A. Palano^{14,d},
 F. Palombo^{22,q}, M. Palutan¹⁹, A. Papanestis⁵¹, M. Pappagallo^{14,d}, L.L. Pappalardo^{17,g},
 W. Parker⁶⁰, C. Parkes⁵⁶, G. Passaleva¹⁸, A. Pastore^{14,d}, G.D. Patel⁵⁴, M. Patel⁵⁵,
 C. Patrignani^{15,e}, A. Pearce⁴⁰, A. Pellegrino⁴³, G. Penso²⁶, M. Pepe Altarelli⁴⁰, S. Perazzini⁴⁰,
 P. Perret⁵, L. Pescatore⁴⁷, K. Petridis⁴⁸, A. Petrolini^{20,h}, A. Petrov⁶⁸, M. Petruzzo^{22,q},
 E. Picatoste Olloqui³⁸, B. Pietrzyk⁴, M. Pikies²⁷, D. Pinci²⁶, A. Pistone²⁰, A. Piucci¹²,
 V. Placinta³⁰, S. Playfer⁵², M. Plo Casasus³⁹, T. Poikela⁴⁰, F. Polci⁸, A. Poluektov^{50,36},
 I. Polyakov⁶¹, E. Polycarpo², G.J. Pomery⁴⁸, A. Popov³⁷, D. Popov^{11,40}, B. Popovici³⁰,
 S. Poslavskii³⁷, C. Potterat², E. Price⁴⁸, J.D. Price⁵⁴, J. Prisciandaro^{39,40}, A. Pritchard⁵⁴,
 C. Prouve⁴⁸, V. Pugatch⁴⁶, A. Puig Navarro⁴², G. Punzi^{24,p}, W. Qian⁵⁰, R. Quagliani^{7,48},
 B. Rachwal²⁷, J.H. Rademacker⁴⁸, M. Rama²⁴, M. Ramos Pernas³⁹, M.S. Rangel², I. Raniuk⁴⁵,
 F. Ratnikov³⁵, G. Raven⁴⁴, F. Redi⁵⁵, S. Reichert¹⁰, A.C. dos Reis¹, C. Remon Alepuz⁶⁹,
 V. Renaudin⁷, S. Ricciardi⁵¹, S. Richards⁴⁸, M. Rihl⁴⁰, K. Rinnert⁵⁴, V. Rives Molina³⁸,
 P. Robbe^{7,40}, A.B. Rodrigues¹, E. Rodrigues⁵⁹, J.A. Rodriguez Lopez⁶⁶, P. Rodriguez Perez^{56,†},
 A. Rogozhnikov³⁵, S. Roiser⁴⁰, A. Rollings⁵⁷, V. Romanovskiy³⁷, A. Romero Vidal³⁹,
 J.W. Ronayne¹³, M. Rotondo¹⁹, M.S. Rudolph⁶¹, T. Ruf⁴⁰, P. Ruiz Valls⁶⁹,
 J.J. Saborido Silva³⁹, E. Sadykhov³², N. Sagidova³¹, B. Saitta^{16,f}, V. Salustino Guimaraes¹,
 C. Sanchez Mayordomo⁶⁹, B. Sanmartin Sedes³⁹, R. Santacesaria²⁶, C. Santamarina Rios³⁹,

M. Santimaria¹⁹, E. Santovetti^{25,j}, A. Sarti^{19,k}, C. Satriano^{26,s}, A. Satta²⁵, D.M. Saunders⁴⁸, D. Savrina^{32,33}, S. Schael⁹, M. Schellenberg¹⁰, M. Schiller⁵³, H. Schindler⁴⁰, M. Schlupp¹⁰, M. Schmelling¹¹, T. Schmelzer¹⁰, B. Schmidt⁴⁰, O. Schneider⁴¹, A. Schopper⁴⁰, K. Schubert¹⁰, M. Schubiger⁴¹, M.-H. Schune⁷, R. Schwemmer⁴⁰, B. Sciascia¹⁹, A. Sciubba^{26,k}, A. Semennikov³², A. Sergi⁴⁷, N. Serra⁴², J. Serrano⁶, L. Sestini²³, P. Seyfert²¹, M. Shapkin³⁷, I. Shapoval⁴⁵, Y. Shcheglov³¹, T. Shears⁵⁴, L. Shekhtman^{36,w}, V. Shevchenko⁶⁸, B.G. Siddi^{17,40}, R. Silva Coutinho⁴², L. Silva de Oliveira², G. Simi^{23,o}, S. Simone^{14,d}, M. Sirendi⁴⁹, N. Skidmore⁴⁸, T. Skwarnicki⁶¹, E. Smith⁵⁵, I.T. Smith⁵², J. Smith⁴⁹, M. Smith⁵⁵, H. Snoek⁴³, I. Soares Lavra¹, M.D. Sokoloff⁵⁹, F.J.P. Soler⁵³, B. Souza De Paula², B. Spaan¹⁰, P. Spradlin⁵³, S. Sridharan⁴⁰, F. Stagni⁴⁰, M. Stahl¹², S. Stahl⁴⁰, P. Stefkova⁵⁵, O. Steinkamp⁴², S. Stemmle¹², O. Stenyakin³⁷, H. Stevens¹⁰, S. Stevenson⁵⁷, S. Stoica³⁰, S. Stone⁶¹, B. Storaci⁴², S. Stracka^{24,p}, M. Stratciuc³⁰, U. Straumann⁴², L. Sun⁶⁴, W. Sutcliffe⁵⁵, K. Swientek²⁸, V. Syropoulos⁴⁴, M. Szczekowski²⁹, T. Szumlak²⁸, S. T'Jampens⁴, A. Tayduganov⁶, T. Tekampe¹⁰, G. Tellarini^{17,g}, F. Teubert⁴⁰, E. Thomas⁴⁰, J. van Tilburg⁴³, M.J. Tilley⁵⁵, V. Tisserand⁴, M. Tobin⁴¹, S. Tolk⁴⁹, L. Tomassetti^{17,g}, D. Tonelli⁴⁰, S. Topp-Joergensen⁵⁷, F. Toriello⁶¹, E. Tournefier⁴, S. Tourneur⁴¹, K. Trabelsi⁴¹, M. Traill⁵³, M.T. Tran⁴¹, M. Tresch⁴², A. Trisovic⁴⁰, A. Tsaregorodtsev⁶, P. Tsopelas⁴³, A. Tully⁴⁹, N. Tuning⁴³, A. Ukleja²⁹, A. Ustyuzhanin³⁵, U. Uwer¹², C. Vacca^{16,f}, V. Vagnoni^{15,40}, A. Valassi⁴⁰, S. Valat⁴⁰, G. Valenti¹⁵, R. Vazquez Gomez¹⁹, P. Vazquez Regueiro³⁹, S. Vecchi¹⁷, M. van Veghel⁴³, J.J. Velthuis⁴⁸, M. Veltri^{18,r}, G. Veneziano⁵⁷, A. Venkateswaran⁶¹, M. Vernet⁵, M. Vesterinen¹², J.V. Viana Barbosa⁴⁰, B. Viaud⁷, D. Vieira⁶³, M. Vieites Diaz³⁹, H. Viemann⁶⁷, X. Vilasis-Cardona^{38,m}, M. Vitti⁴⁹, V. Volkov³³, A. Vollhardt⁴², B. Voneki⁴⁰, A. Vorobyev³¹, V. Vorobyev^{36,w}, C. Voß⁹, J.A. de Vries⁴³, C. Vázquez Sierra³⁹, R. Waldi⁶⁷, C. Wallace⁵⁰, R. Wallace¹³, J. Walsh²⁴, J. Wang⁶¹, D.R. Ward⁴⁹, H.M. Wark⁵⁴, N.K. Watson⁴⁷, D. Websdale⁵⁵, A. Weiden⁴², M. Whitehead⁴⁰, J. Wicht⁵⁰, G. Wilkinson^{57,40}, M. Wilkinson⁶¹, M. Williams⁴⁰, M.P. Williams⁴⁷, M. Williams⁵⁸, T. Williams⁴⁷, F.F. Wilson⁵¹, J. Wimberley⁶⁰, J. Wishahi¹⁰, W. Wislicki²⁹, M. Witek²⁷, G. Wormser⁷, S.A. Wotton⁴⁹, K. Wraight⁵³, K. Wyllie⁴⁰, Y. Xie⁶⁵, Z. Xing⁶¹, Z. Xu⁴¹, Z. Yang³, Y. Yao⁶¹, H. Yin⁶⁵, J. Yu⁶⁵, X. Yuan^{36,w}, O. Yushchenko³⁷, K.A. Zarebski⁴⁷, M. Zavertyaev^{11,c}, L. Zhang³, Y. Zhang⁷, Y. Zhang⁶³, A. Zhelezov¹², Y. Zheng⁶³, X. Zhu³, V. Zhukov³³, S. Zucchelli¹⁵.

¹Centro Brasileiro de Pesquisas Físicas (CBPF), Rio de Janeiro, Brazil

²Universidade Federal do Rio de Janeiro (UFRJ), Rio de Janeiro, Brazil

³Center for High Energy Physics, Tsinghua University, Beijing, China

⁴LAPP, Université Savoie Mont-Blanc, CNRS/IN2P3, Annecy-Le-Vieux, France

⁵Clermont Université, Université Blaise Pascal, CNRS/IN2P3, LPC, Clermont-Ferrand, France

⁶CPPM, Aix-Marseille Université, CNRS/IN2P3, Marseille, France

⁷LAL, Université Paris-Sud, CNRS/IN2P3, Orsay, France

⁸LPNHE, Université Pierre et Marie Curie, Université Paris Diderot, CNRS/IN2P3, Paris, France

⁹I. Physikalisches Institut, RWTH Aachen University, Aachen, Germany

¹⁰Fakultät Physik, Technische Universität Dortmund, Dortmund, Germany

¹¹Max-Planck-Institut für Kernphysik (MPIK), Heidelberg, Germany

¹²Physikalisch-es Institut, Ruprecht-Karls-Universität Heidelberg, Heidelberg, Germany

¹³School of Physics, University College Dublin, Dublin, Ireland

¹⁴Sezione INFN di Bari, Bari, Italy

¹⁵Sezione INFN di Bologna, Bologna, Italy

¹⁶Sezione INFN di Cagliari, Cagliari, Italy

¹⁷Sezione INFN di Ferrara, Ferrara, Italy

¹⁸Sezione INFN di Firenze, Firenze, Italy

¹⁹Laboratori Nazionali dell'INFN di Frascati, Frascati, Italy

²⁰Sezione INFN di Genova, Genova, Italy

²¹Sezione INFN di Milano Bicocca, Milano, Italy

²²Sezione INFN di Milano, Milano, Italy

- ²³Sezione INFN di Padova, Padova, Italy
²⁴Sezione INFN di Pisa, Pisa, Italy
²⁵Sezione INFN di Roma Tor Vergata, Roma, Italy
²⁶Sezione INFN di Roma La Sapienza, Roma, Italy
²⁷Henryk Niewodniczanski Institute of Nuclear Physics Polish Academy of Sciences, Kraków, Poland
²⁸AGH - University of Science and Technology, Faculty of Physics and Applied Computer Science, Kraków, Poland
²⁹National Center for Nuclear Research (NCBJ), Warsaw, Poland
³⁰Horia Hulubei National Institute of Physics and Nuclear Engineering, Bucharest-Magurele, Romania
³¹Petersburg Nuclear Physics Institute (PNPI), Gatchina, Russia
³²Institute of Theoretical and Experimental Physics (ITEP), Moscow, Russia
³³Institute of Nuclear Physics, Moscow State University (SINP MSU), Moscow, Russia
³⁴Institute for Nuclear Research of the Russian Academy of Sciences (INR RAN), Moscow, Russia
³⁵Yandex School of Data Analysis, Moscow, Russia
³⁶Budker Institute of Nuclear Physics (SB RAS), Novosibirsk, Russia
³⁷Institute for High Energy Physics (IHEP), Protvino, Russia
³⁸ICCUB, Universitat de Barcelona, Barcelona, Spain
³⁹Universidad de Santiago de Compostela, Santiago de Compostela, Spain
⁴⁰European Organization for Nuclear Research (CERN), Geneva, Switzerland
⁴¹Institute of Physics, Ecole Polytechnique Fédérale de Lausanne (EPFL), Lausanne, Switzerland
⁴²Physik-Institut, Universität Zürich, Zürich, Switzerland
⁴³Nikhef National Institute for Subatomic Physics, Amsterdam, The Netherlands
⁴⁴Nikhef National Institute for Subatomic Physics and VU University Amsterdam, Amsterdam, The Netherlands
⁴⁵NSC Kharkiv Institute of Physics and Technology (NSC KIPT), Kharkiv, Ukraine
⁴⁶Institute for Nuclear Research of the National Academy of Sciences (KINR), Kyiv, Ukraine
⁴⁷University of Birmingham, Birmingham, United Kingdom
⁴⁸H.H. Wills Physics Laboratory, University of Bristol, Bristol, United Kingdom
⁴⁹Cavendish Laboratory, University of Cambridge, Cambridge, United Kingdom
⁵⁰Department of Physics, University of Warwick, Coventry, United Kingdom
⁵¹STFC Rutherford Appleton Laboratory, Didcot, United Kingdom
⁵²School of Physics and Astronomy, University of Edinburgh, Edinburgh, United Kingdom
⁵³School of Physics and Astronomy, University of Glasgow, Glasgow, United Kingdom
⁵⁴Oliver Lodge Laboratory, University of Liverpool, Liverpool, United Kingdom
⁵⁵Imperial College London, London, United Kingdom
⁵⁶School of Physics and Astronomy, University of Manchester, Manchester, United Kingdom
⁵⁷Department of Physics, University of Oxford, Oxford, United Kingdom
⁵⁸Massachusetts Institute of Technology, Cambridge, MA, United States
⁵⁹University of Cincinnati, Cincinnati, OH, United States
⁶⁰University of Maryland, College Park, MD, United States
⁶¹Syracuse University, Syracuse, NY, United States
⁶²Pontifícia Universidade Católica do Rio de Janeiro (PUC-Rio), Rio de Janeiro, Brazil, associated to ²
⁶³University of Chinese Academy of Sciences, Beijing, China, associated to ³
⁶⁴School of Physics and Technology, Wuhan University, Wuhan, China, associated to ³
⁶⁵Institute of Particle Physics, Central China Normal University, Wuhan, Hubei, China, associated to ³
⁶⁶Departamento de Fisica , Universidad Nacional de Colombia, Bogota, Colombia, associated to ⁸
⁶⁷Institut für Physik, Universität Rostock, Rostock, Germany, associated to ¹²
⁶⁸National Research Centre Kurchatov Institute, Moscow, Russia, associated to ³²
⁶⁹Instituto de Fisica Corpuscular (IFIC), Universitat de Valencia-CSIC, Valencia, Spain, associated to ³⁸
⁷⁰Van Swinderen Institute, University of Groningen, Groningen, The Netherlands, associated to ⁴³

^aUniversidade Federal do Triângulo Mineiro (UFTM), Uberaba-MG, Brazil

^bLaboratoire Leprince-Ringuet, Palaiseau, France

^cP.N. Lebedev Physical Institute, Russian Academy of Science (LPI RAS), Moscow, Russia

^dUniversità di Bari, Bari, Italy

^eUniversità di Bologna, Bologna, Italy

^fUniversità di Cagliari, Cagliari, Italy

^g Università di Ferrara, Ferrara, Italy

^h Università di Genova, Genova, Italy

ⁱ Università di Milano Bicocca, Milano, Italy

^j Università di Roma Tor Vergata, Roma, Italy

^k Università di Roma La Sapienza, Roma, Italy

^l AGH - University of Science and Technology, Faculty of Computer Science, Electronics and Telecommunications, Kraków, Poland

^m LIFAELS, La Salle, Universitat Ramon Llull, Barcelona, Spain

ⁿ Hanoi University of Science, Hanoi, Viet Nam

^o Università di Padova, Padova, Italy

^p Università di Pisa, Pisa, Italy

^q Università degli Studi di Milano, Milano, Italy

^r Università di Urbino, Urbino, Italy

^s Università della Basilicata, Potenza, Italy

^t Scuola Normale Superiore, Pisa, Italy

^u Università di Modena e Reggio Emilia, Modena, Italy

^v Iligan Institute of Technology (IIT), Iligan, Philippines

^w Novosibirsk State University, Novosibirsk, Russia

[†] Deceased